ELSEVIER

Physica C 341–348 (2000) 2079–2082

PHYSICA C

www.elsevier.nl/locate/physc

Fermi Surface Topology of $Bi_2Sr_2CaCu_2O_{8+\delta}$ at $h\nu = 33eV$

Y. -D. Chuang, A. D. Gromko, D. S. Dessau[a] and K. Nakamura, Yoichi Ando[b]

[a]Department of Physics, University of Colorado, Boulder,Colorado, 80309-0390

[b]Central Research Institute of Electric Power Industry (CRIEPI), 2-11-1 Iwato-Kita, Komae, Tokyo 201-8511, Japan

We present Angle-Resolved Photoemission experiments (ARPES) results on $Bi_2Sr_2CaCu_2O_{8+\delta}$ (BSCCO) crystals. With high energy and momentum resolution, we identify the existence of electron-like portions of Fermi Surface (FS) near $\bar{M}$ at $h\nu = 33eV$. This phenomena contrasts with the hole-like topology obtained using $h\nu \approx 22eV$.

1. INTRODUCTION

Among all the normal state properties of high temperature superconductors (HTSC), the Fermi Surface (FS) topology is one of the most important since it needs to be determined prior to correctly predicting many physical properties. The most powerful tool to probe it is Angle-Resolved Photoemission Spectroscopy (ARPES) due to its capability to directly extract energy/momentum relations [1]. Over the past decade, our knowledge on FS topology of HTSC has come mainly from the study of $Bi_2Sr_2CaCu_2O_{8+\delta}$ due to the ideal cleaved surfaces that can be obtained, and the results obtained were widely interpreted as a hole-barrel (no k_z dispersion) centered at the (π, π) or X(Y) points of the Brillouin Zone (see figure 1(a))[2,3]. This result was obtained mainly by using incident photon energies of $h\nu \approx 22eV$ [2]. Recently, we showed that the electronic structure and FS topology appear quite different if measured using $h\nu = 33eV$. In particular, the FS contains electron-like portions near the$(\pi, 0)$ or $(\bar{M})$ points of the Brillouin zone (figure 1(b)) [4]. This new result was confirmed by Feng et al. [5] but then challenged in four recent papers which argued that the electronic structure is hole-like and independent of photon energy [6,7]. They argued that the different spectral behavior observed between $h\nu = 22eV$ and $33eV$ is simply due to strongly $\vec{k}$ dependent matrix element effects, and that the electron-like FS portions were really just superstructure bands from the hole-like topology. They further argued that the energy and momentum resolution used in references [4] and [5] were inadequate to deconvolve all the various effects. Here we present new high resolution ARPES data taken with $h\nu = 33eV$ data which clearly confirms the existence of the electron-like portions of FS. We discuss possible mechanisms by which the topology may very as a function of photon energy.

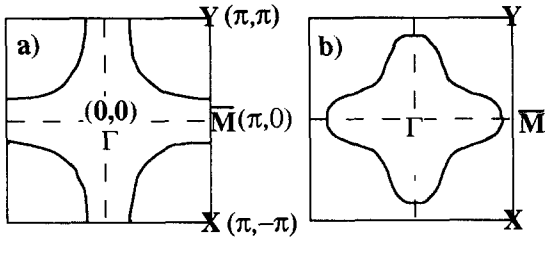

Figure 1. Hole-like FS topology (a) versus electron-like topology (b).

2. EXPERIMENTAL SETUP

The experiments were done at Beamline 10.0.1 at the Advanced Light Source (ALS), Berkeley, CA with a Scienta SES 200 energy analyzer. The angle mode of operation was used to simultaneously collect $\approx$ 89 individual spectra along a 14° angular slice, which was parallel to the θ

PII S0921-4534(00)01066-2

direction, $\Gamma - \bar{M}$ high symmetry line and incident photon polarization. The angular resolution was $(\Delta\theta, \Delta\phi) \approx (0.08^o, 0.25^o)$ and the converted momentum resolution at $h\nu = 33eV$ would be $(\Delta k_x, \Delta k_y) \approx (0.01\pi, 0.03\pi)$. The FS mapping was done by moving either θ (along the 14^o slice) or ϕ (perpendicular to the slice). The energy resolution was better than $10meV$ FWHM from a Au reference at $10K$. The sample Bi046 used in this study was annealed to be overdoped and has $T_c = 79K$. Throughout the experiment, the base pressure was better than $4 * 10^{-11}$ torr and the temperature was maintained at $100K$, well above T_c. All experimental data was normalized by using the high-harmonic emission above E_F.

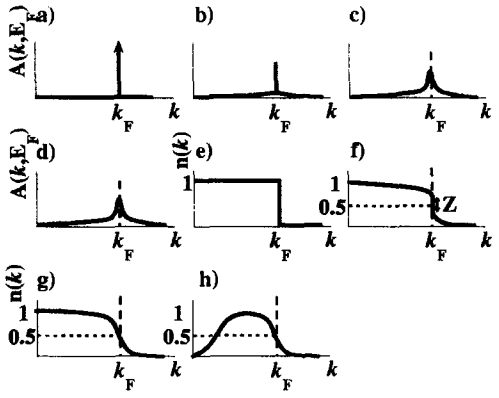

Figure 2. Schematics of the expected behavior of $A(\vec{k}, E_F)$ and $n(\vec{k})$ for a band crossing the FS. (a,e) Non-interacting system at zero temperature. (b,f) Interacting Fermi Liquid with a reduced quasiparticle weight Z. (c,g) Same as (b,f) but with finite energy and momentum resolution. (d,h) Same as (c,g) but including polarization and matrix element effects.

3. RESULTS AND DISCUSSION

In order to analyze ARPES data in more detail, we have previously introduced the criteria which utilize the integrated spectral weight over a small binding energy window centered around E_F, the MAX($A(\vec{k}, E_F)$) method [4]. In figure 2, we show the expected behavior for $A(\vec{k}, E_F)$. Panel (a) shows the zero temperature behavior for a non-interacting electron gas with perfect energy and momentum resolution. We expect there to be a δ-function peak right at E_F due to the infinite lifetime of the excitations. In panel (b) we introduce interactions, which within the Fermi liquid theory framework will reduce the weight of the δ-function peak in $A(\vec{k}, E_F)$ to the amount Z, the quasiparticle weight. In panel (c), we introduce the finite energy and momentum resolution which broadens $A(\vec{k}, E_F)$ and in panel (d),$\vec{k}$-dependent matrix element effects may slowly alter the shape of the curve. Even so, $A(\vec{k}, E_F)$ should still reach its maximum at E_F. A second method is to look at either the 50% point of $n(\vec{k})$ or the maximum of the gradient of $n(\vec{k})$, both of which should occur at E_F (panels (e)-(h) in figure 2). These methods were used in references [4] and [5], and were found to give electron-like FS's for $33eV$ data.

The third method to determine the FS crossing points is to extrapolate the dispersion relation $E(\vec{k})$ up to E_F. This can be conveniently visualized in intensity plots of E vs. $\vec{k}$, as shown in figure 3(a), which presents T=100K ARPES data from overdoped $Bi_2Sr_2CaCu_2O_{8+\delta}$. Panel (a) shows some grey-color scale EDCs, the vertical axes of which are the binding energy (eV), and the horizontal axes the θ angle, with 0^o equal to normal emission. The grey scale is shown on top with the maximum, Max, and the minimum, Min. In order to highlight detailed features, each plot is further normalized separately to its maximum value thus the intensity cannot be connected between plots. Each plot was taken at a different ϕ angle, with it's location in the Brillouin zone indicated by the (i)-(v) in panel (c). Each of these plots shows one or more features which disperse in energy as a function of angle. Most of these features can be easily followed up to E_F. Main band will be indicated by M and superstructure band by S.S. Due to polarization selection rules [1], superstructure (S.S.) bands might have stronger emission than the main band in certain $\vec{k}$ space region (see panel(v)). In figures 3(b) and 3(c) we use white dots to indicate FS crossing points determined by looking at the dispersion in part (a). We see that the white dots can be nat-

urally connected by electron-like portions of FS (thick black line) plus superstructure bands (thin black line). In contrast, the hole-like FS topology in panel (c) cannot explain many of the crossing location.

Another way to visualize FS crossings is to make a two-dimensional $A(\vec{k}, E_F)$ plot versus $\vec{k}$, as shown in figures 3(b) and 3(c) for a portion of the $(\Gamma - \bar{M} - Y)$ quadrant. The location of this portion is indicated by the hatched area in schematic FS plot next to the grey scale. Now the relative intensity scales between 11 (5 are shown in 3(a)) individual panels are set to be the same in order to compare each other. They are first normalized by looking at the high-harmonic emission above E_F only. To make $A(\vec{k}, E_F)$, we then integrate the spectral weight of the 11 EDCs over a $(-25meV, 25meV)$ energy window. The FS should show up on these contour plots as the maximum spectral intensity locus. The very clear match in panel (b) between the white dots, black lines and high intensity locus indicates that the FS determined by using both the dispersion and $A(\vec{k}, E_F)$ plots give a self-consistent result which matches the electronlike FS topology proposed by us earlier [4]. The 50% point or max gradient of $n(\vec{k})$ plots additionally have been found to be consistent with this topology.[4,5].

The $33eV$ data presented by Fretwell et al.[6] is very similar to our data of figure 3(b), and we have found their data to also be consistent with the electron-like FS topology. However, they have argued that their data is better fit by a hole-like topology, which we have overlayed on our data in figure 3(c). The thick black line is the main band FS while all other lines are S.S. or "shadow band" derived FS. The dashed portions indicate the region of reduced spectral weight empirically introduced to help explain the data. Even with this extra degree of freedom, this topology can not explain the data in a number of ways: (1) It can not explain the extra emission nor the FS curvature around the angle $(14, 2)$. (2) It cannot naturally explain the experimental emission in the region in around angle $(19, 5)$. The only possibility is to argue with shadow band. However this is unlikely due to the very small expected intensity of this feature (shadow of a superstructure with unfavorable matrix elements effect (dashed)). It is impossible due to the backwards dispersion that a shadow band must have, while the experimental band has a forward dispersion relation, as shown in panel (iii) of figure 3(a).

The increased energy and momentum resolution bring up other subtleties which have not been previously observed. In figure 3(b), if we track the main electron-like FS from the $\Gamma - Y$ line towards the $\Gamma - \bar{M}$ line, the intensity first gets greater and then it gets weaker around $(14, 2)$ before getting stronger again along the $\Gamma - \bar{M}$ line. This makes the FS appear as if it has two components - one nearer the $\Gamma - Y$ line and one nearer the $\Gamma - \bar{M}$ line. Further study needs to be carried out to deconvolve the origin of the separation of the FS into these components, as well as to study potential differences in the behavior of each component.

An obviously critical issue we are left with is how to connect the electron-like FS topology observed at $33eV$ with the hole-like topology observed at lower photon energies. A natural possibility is to consider coherent three-dimensional band structure effects, although this would need to be reconciled with the highly two-dimensional nature of the cuprates. An even-odd splitting between the CuO_2 bilayer may produce both an electron and a hole like FS in the same sample, but both topologies also show up in single-layer Bi2201 data [4]. Two FS's may simultaneously exist in the same sample for other reasons as well, for instance due to phase separation into hole-rich and hole-poor regions or into regions with and without stripe disorder [5], each of which may produce its own FS portions. Within these scenarios we still need to understand why one piece of the FS is accentuated at one photon energy while another is accentuated at another, an issue in which matrix element effects [8] may play a significant role.

4. CONCLUSION

In this proceeding, we have presented high energy and momentum resolution ARPES results on the normal state of overdoped $Bi_2Sr_2CaCu_2O_{8+\delta}$ at $h\nu = 33eV$. We clearly

identify the existence of electron-like portions of Fermi Surface near $\bar{M}$ by looking at the high intensity locus in $A(\vec{k}, E_F)$ plots as well as the dispersion of EDCs. We reach the same result by looking at either the main band or the superstructure bands. In contrast, the holelike topoloy obtained from $22eV$ data cannot explain the details of these spectra, even with the ad-hoc inclusion of strong $\vec{k}$-dependent matrix element effects. In addition, our increased reolution shows some new and potentially important subtleties to the data including a break in the main FS.

This work was partially supported by the ONR and was performed at the Advanced Light Source, Berkeley which is supported by the DOE.

REFERENCES

1. For a review, see Z.-X. Shen, D.S. Dessau, Phys. Rep. **253**, 1 (1995)
2. K. Gofron *et al.*, Phys. Rev. Lett. **73**, 3302 (1994); D.M. King *et al.*, Phys. Rev. Lett. **73**, 3298 (1994); H. Ding *et al.*, Phys. Rev. B **54**, R9678 (1996); A.G. Loeser *et al.*, Science **273**, 325 (1996); D.S. Marshall *et al.*, Phys. Rev. Lett. **76**, 4841 (1996); H. Ding *et al.*, Nature **382**, 51 (1996); H. Ding *et al.*, Phys. Rev. Lett. **76**, 1533 (1996); Jian Ma *et al.*, Phys. Rev. B **51**, 3832 (1995); P. Aebi *et al.*, Phys. Rev. Lett. **72**, 2757 (1994).
3. N.L. Saini *et al.*, Phys. Rev. Lett. **79**, 3467 (1997)
4. Y.-D. Chuang *et al.*, Phys. Rev. Lett. **83**, 3717 (1999)
5. D.L. Feng *et al.*, cond-mat/9908056
6. H.M. Fretwell *et al.*, cond-mat/9910221; J. Mesot *et al.*, cond-mat/9910430.
7. S.V. Borisenko *et al.*, cond-mat/9912289; M.S. Golden *et al.*, cond-mat/9912332.
8. A. Bansil *et al.*, Phys. Rev. Lett. **83**, 5154 (1999)

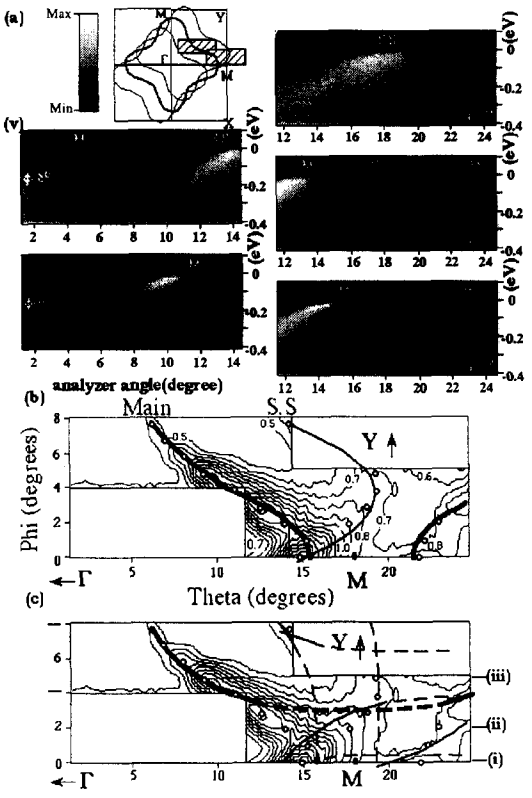

Figure 3. (a) E vs. $\vec{k}$ plots from overdoped Bi2212 sample Bi046 measured at $100K$. Vertical axes are binding energy (eV) and horizontal axes are the angle θ, with normal emission at $\theta = 0^o$. The location of each cut in the $(\Gamma - \bar{M} - Y)$ quadrant of the Brillouin zone is shown in panel (c). Main bands are labeled by M and superstructure band by S.S. The intensity scale is shown on top. Panels (b) and (c) are contour plots of the spectral intensity at E_F. BZ location of contour plot is indicated by the hatched area in schematic FS plot. The increment of each contour line is 0.1 and minimum is 0.5. White dots are the FS crossings determined from part (a). Panel (b) shows the agreement with the electron-like topology while panel (c) shows the disagreement with the hole-like topology.